CANCOM2024 – CANADIAN INTERNATIONAL CONFERENCE ON COMPOSITE MATERIALS

CHARACTERIZATION OF 3D-PRINTED BAMBU PAHT-CF COMPOSITE

Elsafty, AA[1], Elbanna, H[1], Elruby, AY[1]*, and Nakhla, S[1]
[1] Department of Mechanical Engineering, Memorial University, St. John's, NL, Canada
* Corresponding author (aelruby@mun.ca)

Keywords: *3d printed composite, Digital image correlation, Printing direction*

ABSTRACT

This research aims to characterize the mechanical properties of the Bambu PAHT-CF composite. This is a printed composite of Nylon PA12 and carbon fiber that is typically printed using Bambu Lab X1 Carbon 3D printer. Therefore, this work includes studying the effects of printing direction on the mechanical properties and its impact on the final part's tensile and failure behaviors. For this purpose, dog bone specimens are fabricated as per ASTM D638 having an octagram spiral infill pattern with a layer thickness of 0.2 mm. Half of the specimens are oriented vertically on the build plate, while the remaining half are placed horizontally with their narrow faces resting on the build plate. Tensile test is conducted as per ASTM D638, thus a strain rate of 5 mm/min is applied by the Instron 5585H tensile test machine. GOM Correlate software is used for digital image correlation (DIC) and 3D motion analysis of the specimens during testing to record strain measurements and conclude the stress and strain behavior.

1 INTRODUCTION

Recently, the demand for 3D printing due to rapid technological development has resulted in a reduction in production costs and material waste. Additionally, it enabled the fabrication of complex geometries, justifying its use in many areas of aerospace, construction and civil engineering, biomedical engineering and robotics [1]. One process that has been extensively utilized in the manufacture of polymeric 3D printed parts is Fused Deposition Modeling (FDM). FDM is a layer-by-layer, additive manufacturing process based on a computer-aided design (CAD). A polymeric filament material is extruded through a heated nozzle and deposited in a semi-molten state in order to create the desired shape. The structure is manufactured by the sequential build-up of these layered depositions, each new layer fusing with material that has already been deposited [2][3]. The most commonly used thermoplastic polymers in the FDM process are polylactic acid (PLA), acrylonitrile butadiene styrene (ABS), polyamide 12 (PA 12), and polyethylene terephthalate glycol (PETG) [4]. The quality of the 3D-printed composite is primarily dependent on its mechanical properties, and the layering process usually results in undesired material imperfections [6]. Numerous parameters affect the mechanical properties of 3D printed composites, such as build orientation, infill density, layer thickness, temperature and feed rate [1]. Accordingly, this study investigates the effect of the build orientation on the mechanical properties of Bambu PAHT-CF composite in a quest to determine which orientation will result in optimal mechanical properties. PAHT-CF is a printed composite of Nylon PA12 and carbon fiber printed using Bambu Lab X1 Carbon 3D printer with an octagram spiral infill pattern with a layer thickness of 0.2 mm.

2 SPECIMEN PREPARATION

Flat standard tensile PAHT-CF specimens were fabricated as per the ASTM D638-22 [5], adhering to its recommended dimensions for type 1 where sufficient material having a thickness of 7 mm or less is available, as illustrated in the schematic diagram in Figure 1 and Table 1. Two distinct batches, denoted as A and B, were acquired for the samples used in the tensile tests where each batch consists of ten specimens. The samples were categorized into two groups within each batch: the first group, labelled TV1-5 A or B, were oriented vertically on the build plate in the upward z-direction. In contrast, the second half of the specimens, identified as TH6-10 A or B, were placed horizontally with their narrow faces resting on the build plate, as illustrated in Figure 2.

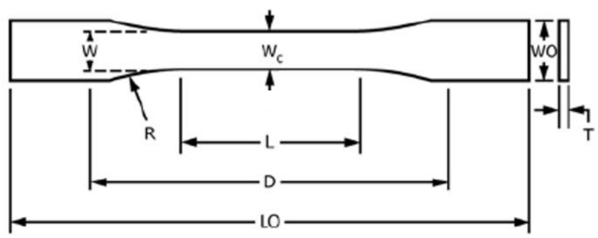

Figure 1: Flat (rectangular) specimen geometry (ASTM D638-22) [5].

Table 1: Flat specimen geometry (ASTM D638-22).

Dimensions [mm]		
Width of Narrow Section	W	13.0
Width Overall	Wo	19.0
Length of Narrow Section	L	57.0
Length	LO	165.0
Thickness	T	3.2
Radius of Fillet	R	76.0

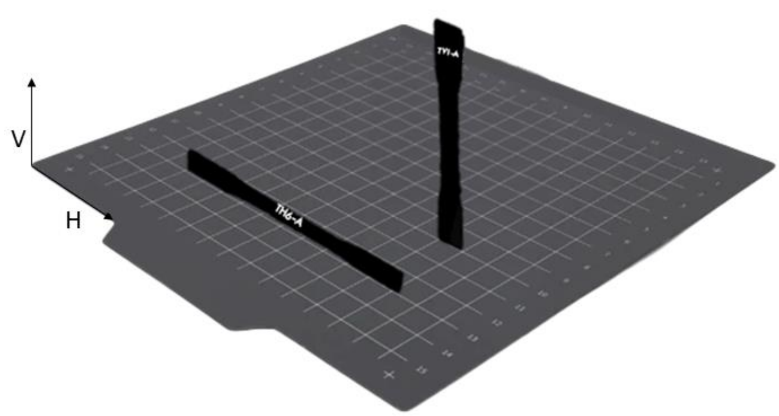

Figure 2: Specimens vertical and horizontal printing orientation on the building plate.

3 TENSILE TESTING SETUP

The tensile test specimens are mechanically characterized in an electromechanical load frame, namely, Instron 5585H, with a maximum loading capacity of 250 kN to apply the tensile load with a strain rate of 5 mm/min according to ASTM D638. Following standard testing procedures, specimens are fixed from one end while a monotonic displacement was applied on the other. The load frame is equipped with a 3D digital image correlation (DIC) stereo system focused on capturing strain measurements in the y-direction. The DIC system used consists of two Mega Speed highspeed cameras, model MS 130K, and LED lights working in sync to capture full-field strain data. The sensor pixel size of the identical cameras is 12 µm. The 40 mm lenses are used to provide excellent focus on the specimens. The intention behind this setup is to imitate the capabilities of the human vision system. By doing so, we aim to not only measure the strain in a specific direction but also to capture the entire 3D strain field of the model. This approach provides a complete understanding of the material's behavior under tension and enables a comprehensive analysis of its mechanical response. The load frame with the stereo camera system is shown in Figures 3a and 3b. The 3D DIC system is calibrated using GOM correlate standard coded panel MV 55x44. The 3D version of GOM correlate software 2017© is used for the analysis [6]. Given that the material under investigation is 3D printed, there is a potential risk of the specimen absorbing the spray paint used for speckling. This absorption could introduce errors when defining and verifying the speckle pattern, so precautionary measures are taken to avoid this issue. Consequently, a layer of clear paint is carefully applied to all samples before the standard speckling process. This clear paint acted as a protective barrier, serving to prevent the absorption of the subsequent spray paint used for speckling. The clear paint layer is allowed to dry thoroughly before proceeding with the normal speckling process. Subsequently, the specimens are speckled using black and white paint by layering one color on top of the other until the required density is achieved, as illustrated in Figure 4.

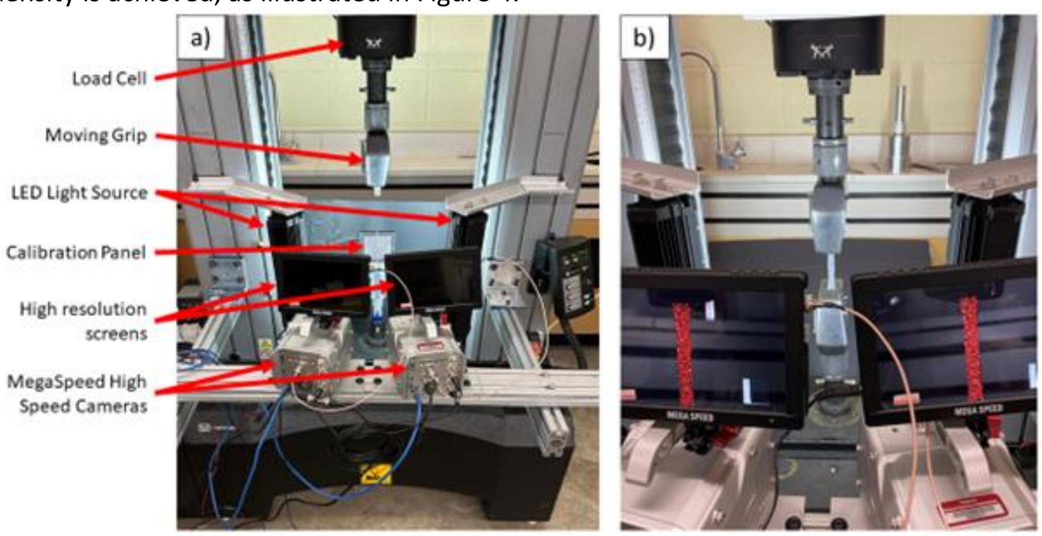

Figure 3: Test setup: a) Instron 5585H load frame with high-speed stereo system for 3D digital image correlation (3D-DIC) b) Tensile testing setup.

4 TENSILE TESTING RESULTS

Full-field longitudinal strain measurements just before the final fracture and separation of tensile specimen for specimen TV4-A, which is oriented vertically and TH7-A, which is horizontally oriented, are shown in Figures 4a and

4b, respectively. Load values were obtained from the Instron 5585H load cell, while displacement measurements were attained using the GOM software. Accordingly, the generated stress-strain curves for batches A and B provided in Figures 5a and 5b were used to evaluate the specimens' mechanical behavior. Studying the stress-strain curves provided valuable insights into the behavior of the samples, as detailed in Tables 2 and 3. The analysis involved determining mechanical properties, including modulus of elasticity, yield stress, ultimate stress, and ultimate strain recorded at the onset of fracture.

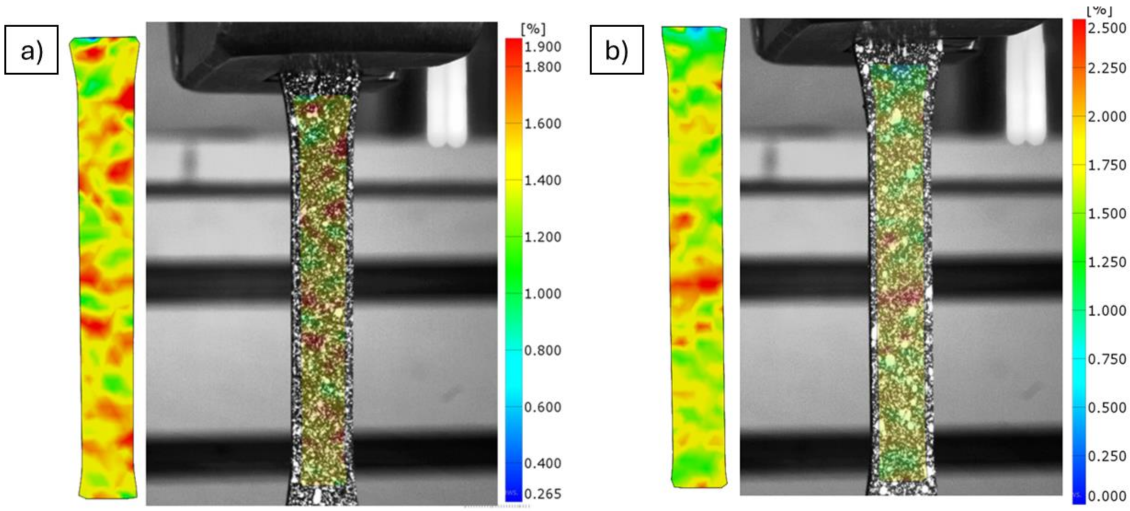

Figure 4: a) Full-field longitudinal strain of specimen TV4-A just before failure, b) Full-field longitudinal strain of specimen TH7-A just before failure.

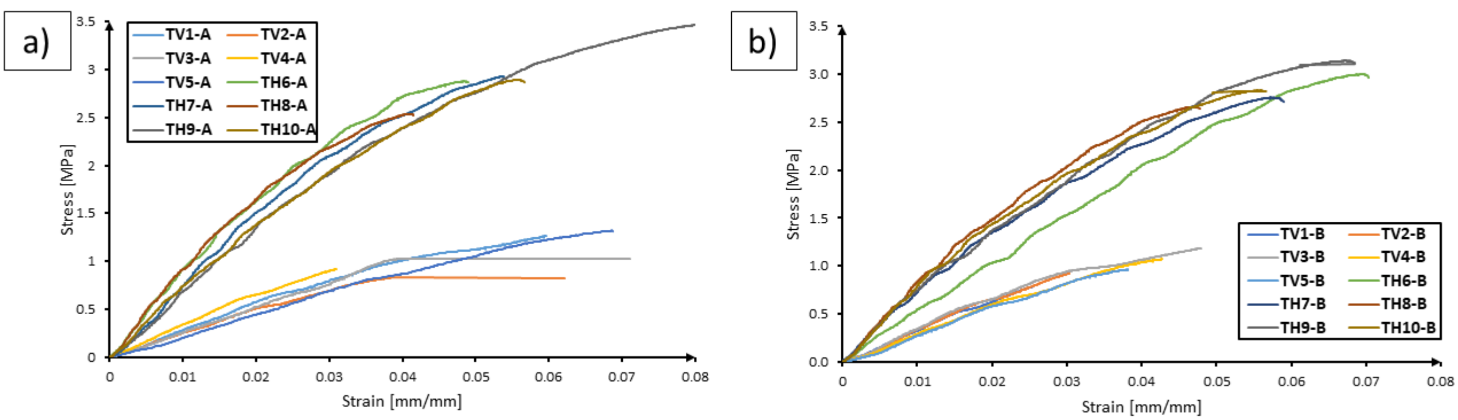

Figure 5: Engineering stress-strain behavior of a) batch A and b) batch B.

Table 2. Batch-A mechanical properties reported from testing.

Specimen	Modulus of Elasticity (MPa)	Yield Stress (MPa)	Ultimate Stress (MPa)	Ultimate Strain (mm/mm)
TV1-A	30.690	0.671	1.266	0.060

TV2-A	25.372	0.606	0.828	0.062
TV3-A	27.801	0.677	1.028	0.071
TV4-A	27.206	0.702	1.023	0.041
TV5-A	24.976	0.872	1.319	0.069
TH6-A	87.250	1.730	2.876	0.049
TH7-A	81.415	1.570	2.930	0.054
TH8-A	90.408	1.732	2.538	0.041
TH9-A	63.085	2.173	3.221	0.083
TH10-A	67.345	1.792	2.741	0.057

Table 3. Batch-B mechanical properties reported from testing.

Specimen	Modulus of Elasticity (MPa)	Yield Stress (MPa)	Ultimate Stress (MPa)	Ultimate Strain (mm/mm)
TV1-B	37.513	0.531	0.782	0.025
TV2-B	25.372	0.641	0.926	0.030
TV3-B	33.219	0.948	1.187	0.048
TV4-B	30.773	0.691	1.072	0.043
TV5-B	29.766	0.636	0.962	0.038
TH6-B	50.741	2.524	2.999	0.071
TH7-B	73.115	1.383	2.757	0.060
TH8-B	85.078	1.405	2.659	0.048
TH9-B	76.338	1.225	3.143	0.069
TH10-B	81.888	1.386	2.832	0.057

The graphs above illustrate the different responses of samples printed horizontally and vertically when subjected to tensile loads. Specifically, samples TH6-10-A, created with a flat horizontal orientation on the build plate, display a remarkable ability to withstand higher tensile loads compared to samples TV1-5-A, which were printed upright. For horizontally oriented samples, the mean tensile strength and Young's modulus were 1.79 ± 0.2 MPa and 77.9 ± 12.1 MPa respectively. On the other hand, in the vertically oriented samples, the values are 0.71 ± 0.1 MPa and 27.2 ± 2.28 MPa. This disparity suggests that specimens with a horizontal orientation exhibit significantly greater toughness, responding more effectively and enduring nearly double the applied tensile loads compared to their upright counterparts. Batch B displayed similar behavior to the first batch, mirroring the trend observed in the initial set of specimens. Notably, specimens TH6-10-B exhibited greater resistance to tensile loads when compared to samples TV1-5-B.

5 TENSILE SAMPLES FRACTOGRAPHY

Examining the manufacturing defects provides insight and understanding of the mechanical response of samples. Therefore, the fracture surface under the 5MP Edge AM7915MZT Dino-Lite digital microscope is shown in Figure 6. Figure 6a shows sample TV4-A, characterized by the existence of voids. These voids are formed because the sample is printed with two outline layers with a total thickness of 0.4 mm and then filled from the inside. Figure 6B shows sample TH7-A with fewer voids. Therefore, the effect of voids is clearly demonstrated when comparing the mechanical properties of both orientations.

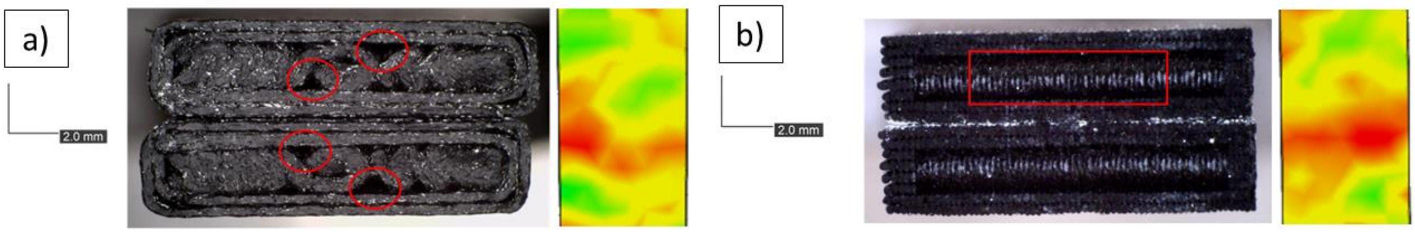

Figure 6: Fracture surface under microscope for a) TV4-A and b) TH7-A.

6 CONCLUSION

This work presents selected results from an extensive testing program for 3D printed Bambu PAHT-CF composite according to ASTM D638 for tensile (type I). The main objective of the study was to identify the effect of printing orientation on the mechanical properties and its impact on the final part's tensile and failure behaviors. Digital image correlation (DIC) was employed to get full-field surface-strain measurements. It can be concluded that the tensile strength, failure strain and modulus of Bambu Lab X1 Carbon 3D printer-printed rectangular specimens were shown to be anisotropic depending on build orientation. The tensile strength of the 3D-printed PAHT-CF composite decreased by around 30% when the printing orientation was altered from horizontal to vertical due to the increase in voids.

7 REFERENCES

[1] Gonabadi, H., Yadav, & A., & Bull, S. J. "The effect of processing parameters on the mechanical characteristics of PLA produced by a 3D FFF printer". *The International Journal of Advanced Manufacturing Technology,* Vol. 111, no. 3, pp 695–709, 2020. https://doi.org/10.1007/s00170-020-06138-4.

[2] Zaldivar, R. J., Witkin, D. B., McLouth, T., Patel, D. N., Schmitt, K., & Nokes, J. P. "Influence of processing and orientation print effects on the mechanical and thermal behavior of 3D-Printed ULTEM ® 9085 Material". *Additive Manufacturing*, Vol. 13, pp 71–80, 2017. https://doi.org/10.1016/j.addma.2016.11.007.

[3] Hoon Ahn, S., Baek, C., Lee, S., & Shup Ahn, I. "ANISOTROPIC TENSILE FAILURE MODEL OF RAPID PROTOTYPING PARTS-FUSED DEPOSITION MODELING (FDM)". *International Journal of Modern Physics B*, Vol. 17, pp 1510–1516, 2003. https://doi.org/10.1142/S0217979203019241.

[4] Tanabi, H. "Investigation of the shear properties of 3D printed short carbon fiber-reinforced thermoplastic composites". *Journal of Thermoplastic Composite Materials*, Vol. 35, pp 2177–2193, 2022. https://doi.org/10.1177/08927057211063399

[5] ASTM D638-22. "Standard Test Method for Tensile Properties of Plastics", 2022. https://www.astm.org/d0638-22.html

[6] Elruby, A. Y., Oldford, D., & Quinton, B. W. T. "In-service effects on mechanical and fracture properties of steel from the arctic drilling unit kulluk". *SNAME Maritime Convention*, p 106, 2022. https://doi.org/10.5957/SMC-2022-106.